We are IntechOpen,
the world's leading publisher of
Open Access books
Built by scientists, for scientists

6,900
Open access books available

185,000
International authors and editors

200M
Downloads

Our authors are among the

154
Countries delivered to

TOP 1%
most cited scientists

12.2%
Contributors from top 500 universities

BOOK CITATION INDEX
CLARIVATE ANALYTICS
INDEXED

WEB OF SCIENCE™

Selection of our books indexed in the Book Citation Index
in Web of Science™ Core Collection (BKCI)

Interested in publishing with us?
Contact book.department@intechopen.com

Screening and Evaluating Environmentally-Friendly Corrosion Inhibitors for Amine-Based CO$_2$ Absorption Process

Sureshkumar Srinivasan, Amornvadee Veawab and Adisorn Aroonwilas

Additional information is available at the end of the chapter

Abstract

This chapter evaluated the performance of environmentally friendly organic corrosion inhibitors on carbon steel in the amine-based carbon dioxide (CO$_2$) absorption process. The evaluation was experimentally conducted using electrochemical techniques in 5.0 kmol/m^3 monoethanolamine (MEA) solutions in the absence and presence of process contaminants, namely formate and chloride, at 80°C and 0.55 mol/mol CO$_2$ loading. The results show, in the absence of process contaminants, that 2-aminobenzene sulfonic acid, 3-aminobenzene sulfonic acid, 4-aminobenzene sulfonic acid, sulfapyridine, and sulfolane yielded 85–92% corrosion inhibition efficiencies, while sulfanilamide yielded the lowest efficiency of 20–42%. Sulfolane was the only tested inhibitor whose performance could be maintained in chloride- and formate-containing MEA solutions. On the contrary, the performance of 3-aminobenzene sulfonic acid and sulfapyridine was decreased by chloride. The performance of all the tested aminobenzene sulfonic acids was compromised by formate.

Keywords: corrosion inhibitor, CO$_2$ capture, CO$_2$ absorption, gas treating, alkanolamine, electrochemical tests, carbon steel

1. Introduction

Corrosion is one of the most severe operational problems in a typical amine-based carbon dioxide (CO$_2$) absorption process [1]. To mitigate corrosion, a number of organic and inorganic corrosion inhibitors have long been applied to the process. The corrosion inhibitors that were found effective are those containing heavy metals such as vanadium-, antimony-, cobalt-,
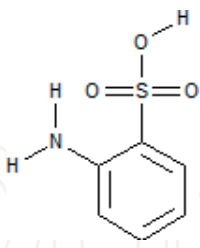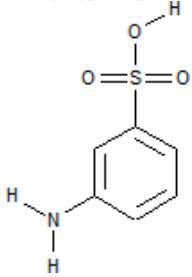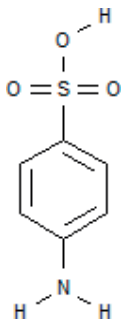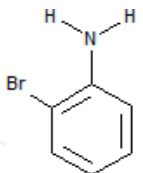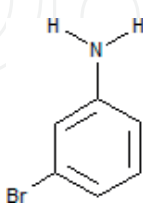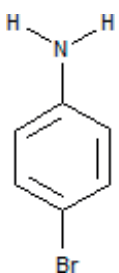
and nickel-based compounds. For example, 0.05–0.10% sodium metavanadate and antimony tartrate were reported to yield 90–95% inhibition efficiency (IE) when used in 15–30% mono-ethanolamine (MEA) solution for mild steel in the ammonia plant [2]. A mixture of sodium metavanadate and cobalt nitrate and a mixture of ammonium metavanadate and amines performed well on mild steel in 50% MEA solution in acid gas treating process. They reduced corrosion rates (CRs) of mild steel down to less than 1 mile per year [3]. A combination of copper carbonate, dihydroxyethyl glycine, alkali metal thiocyanate, ammonium permanganate, and nickel or bismuth oxide provided 99% of inhibition efficiency for the MEA-based acid gas treating plants using mild steel [4]. A mixture of 50 ppm thiocyanate and 100 ppm bismuth citrate was reported to significantly reduce the corrosion of mild steel, stainless steel (304 and 316), and monel with approximately 94% in the natural gas treating plants using 30% MEA solution [5]. Dodecylbenzyl chloride with alkyl pyridine and nickel acetate was successfully applied with 93% efficiency in natural gas treating plants using 20-60% diethanolamine (DEA) solutions [6]. A mixture of amino ethyl piperazine, formaldehyde-thiourea, polymer and nickel sulfate yielded close to 100% efficiency on carbon steel in 30% MEA solution in the refinery gas conditioning unit [7]. More reviews on the corrosion inhibitors used for the amine-based CO_2 absorption process can be found in [8].
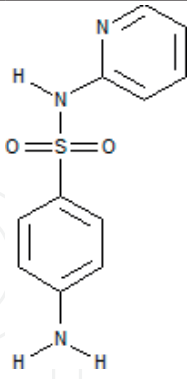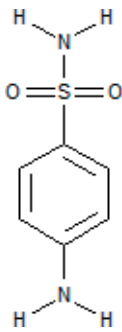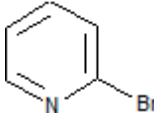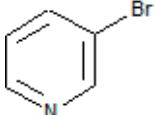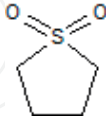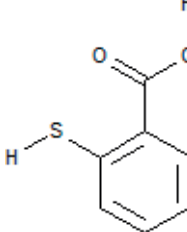
Despite their inhibition effectiveness, the usage of some heavy metal inhibitors is now restricted while others would be banned in the near future due to incoming stringent environmental regulations on the use of toxic chemicals. The objective of this chapter is thus to search for an environmentally friendly corrosion inhibitor with comparable inhibition performance that can replace conventional highly toxic corrosion inhibitors for the CO_2 absorption process. To achieve such an objective, a number of organic compounds were selected as potential corrosion inhibitors based on the principles of Hard and Soft Acids and Bases (HSAB), toxicity properties, and quantum chemical analysis. The inhibition performance of the selected inhibitors on carbon steel was experimentally tested using electrochemical techniques under a test condition simulating the process solution environment, that is, 5.0 kmol/m³ monoethanolamine (MEA) solution at 80°C and 0.55 mol/mol CO_2 loading. The effects of the corrosion inhibitor concentration and process contaminants (namely, formate and chloride) on the inhibition performance were also studied.

2. Selection of tested corrosion inhibitors

2.1. Compound selection

The principle of Hard and Soft Acids and Bases (HSAB) was employed as the first screening criteria to select the corrosion inhibitors to be tested. Since ferrous iron (Fe^+) which is a borderline acid is typically found in the amine-based CO_2 absorption process [1, 9], eight aniline- and two pyridine-based compounds which are the borderline basic inhibitors were the preferred choices. As shown in **Table 1**, the aniline compounds, including 2-, 3-, 4-aminobenzene sulfonic acids, sulfanilamide, and sulfapyridine, contain nitrogen (N), sulfur (S), and oxygen (O) as the reaction centers for adsorption, while 2-, 3-, 4-bromoaniline and bromopyridine contain N and bromine (Br).

Compound	Formula	Structure[a]
Aniline-based compounds		
2-aminobenzene sulfonic acid	C$_6$H$_7$NO$_3$S	
3-aminobenzene sulfonic acid	C$_6$H$_7$NO$_3$S	
4-aminobenzene sulfonic acid	C$_6$H$_7$NO$_3$S	
2-bromoaniline	C$_6$H$_6$BrN	
3-bromoaniline	C$_6$H$_6$BrN	
4-bromoaniline	C$_6$H$_6$BrN	

Compound	Formula	Structure[a]
Sulfapyridine	$C_{11}H_{11}N_3O_2S$	
Sulfanilamide	$C_6H_8N_2O_2S$	
Pyridine-based compounds		
2-bromopyridine	C_5H_4BrN	
3-bromopyridine	C_5H_4BrN	
Sulfur-based compounds		
Sulfolane	$C_4H_8O_2S$	
Thiosalicylic acid	$C_7H_6O_2S$	

[a]Molecular structures redrawn from PubChem database [PubChem[1]].

Table 1. List of selected compounds.

In addition to the abovementioned compounds, two sulfur-containing compounds, namely sulfolane and thiosalicylic acid, were also chosen since they were reported to be effective due to their superior electron-donating ability compared to nitrogen and oxygen [10–12]. Sulfolane is a heterocyclic compound with a sulfonyl reaction center. Thiosalicylic acid has one S- and two O-reaction centers.

2.2. Toxicity evaluation

The selected compounds were first screened based on compound toxicity using the criteria in that the corrosion inhibitors must not be more toxic than the absorbents used in the CO_2 absorption process. That is, their lethal dosage (LD_{50}) values must be equal or greater than those of the absorbents. Since MEA is the benchmark absorbent for the amine-based CO_2 absorption process, its toxicity value was used as the basis for comparison. Thus, any compound having LD_{50} (oral rat) less than LD_{50} of MEA (1720 mg/kg) was removed from the list of selected compounds to be tested. Note that, in addition to LD_{50} values, carcinogenicity and hazard rating for toxicity were also used for compound screening when toxicity information was not available.

Table 2 shows that 4-bromoaniline and 2-bromopyridine have LD_{50} lower than MEA, and all bromine (Br⁻ substituted) compounds are suspected carcinogens with hazard ratings of 3 (moderate hazard). This indicates greater toxicity and health risk of these compounds compared to other selected compounds. As a result, these bromine compounds (i.e., 2-bromoaniline, 3-bromoaniline, 4-bromoaniline, 2-bromopyridine, and 3-bromopyridine) were removed from the list of tested inhibitors. Seven remaining compounds were selected for further

Inhibitor	LD_{50} (oral rat) mg/kg	Carcinogenicity	Hazard rating for toxicity[b]
2-aminobenzene sulfonic acid	—	—	0
3-aminobenzene sulfonic acid	—	—	2
4-aminobenzene sulfonic acid	12,300	—	0
Sulfapyridine	15,800	—	2
Sulfanilamide	—	—	2
2-bromoaniline	—	Suspected carcinogens	3
3-bromoaniline	—	Suspected carcinogens	3
4-bromoaniline	456	Suspected carcinogens	3
2-bromopyridine	92	Suspected carcinogens	3
3-bromopyridine	—	Suspected carcinogens	3
Sulfolane	1941	—	2
Thiosalicylic acid	—	—	0

[a]All details were extracted from MSDS of each compound [chemwatch, 2012].
[b]Hazard ratings in a scale of 0–4 (0, min/nil; 1, low; 2, moderate; 3, high and 4, extreme).

Table 2. Toxicity information of the selected corrosion inhibitors[a].

Compound	E_{HOMO} (eV)	ΔN	Z
2-aminobenzene sulfonic acid	−9.17	0.25	2.54
3-aminobenzene sulfonic acid	−9.10	0.25	2.45
4-aminobenzene sulfonic acid	−9.45	0.22	2.48
Sulfanilamide	−9.18	0.25	2.52
Sulfapyridine	−9.01	0.27	2.56
Thiosalicylic acid	−9.27	0.21	−0.18
Sulfolane	−10.82	0.18	2.44

Table 3. Quantum chemical parameters of selected compounds.

analysis, that is, 2-aminobenzene sulfonic acid, 3-aminobenzene sulfonic acid, 4-aminobenzene sulfonic acid, sulfapyridine, sulfanilamide, sulfolane, and thiosalicylic acid.

2.3. Quantum chemical analysis

Quantum chemical analysis was carried out to predict the inhibition performance of selected compounds prior to corrosion tests. This was done to eliminate the selected compounds with the predicted inhibition performance that was much poorer than others. The analysis was carried out using the semiempirical quantum chemistry calculations package MOPAC2007 to perform the parameterization (PM-6) calculations [13]. The quantum parameters of interest included the highest occupied molecular orbital energy (E_{HOMO}), fraction of electron transferred (ΔN), and charge of the donor atom (Z). These parameters relate directly to the inhibition efficiency [10, 12, 14–16]. The results in **Table 3** show that E_{HOMO}, ΔN, and Z values of all selected compounds are in comparable ranges, suggesting comparable inhibition performance. Sulfapyridine has the highest E_{HOMO}, ΔN, and Z, implying that sulfapyridine might be the most efficient inhibitor compared to others. Thus, no selected compounds should be removed from the list.

3. Experiments

3.1. Experimental setup

Figure 1 illustrates the experimental setup used for electrochemical corrosion tests. It comprises a microcell, a water bath, a gas supply set, a water-cooled condenser, and a potentiostat. The microcell was a 100-ml three-electrode corrosion cell consisting of a cylindrical working electrode, a silver/silver chloride (Ag/AgCl) reference electrode, and a platinum counter electrode. The water bath with a temperature controller was used to control the temperature of the corrosion cell at a required temperature. The gas supply set consisted of CO_2 and nitrogen (N_2) cylinders with gas regulators and flow meters. The water-cooled condenser was used for minimizing evaporation losses from the corrosion cell. The potentiostat was PAR 263A (Princeton Applied Research, USA) interfaced with an impedance system (Model 5210 Lock-in amplifier). The Powercorr (Version 2.53) software was used to record and analyze the
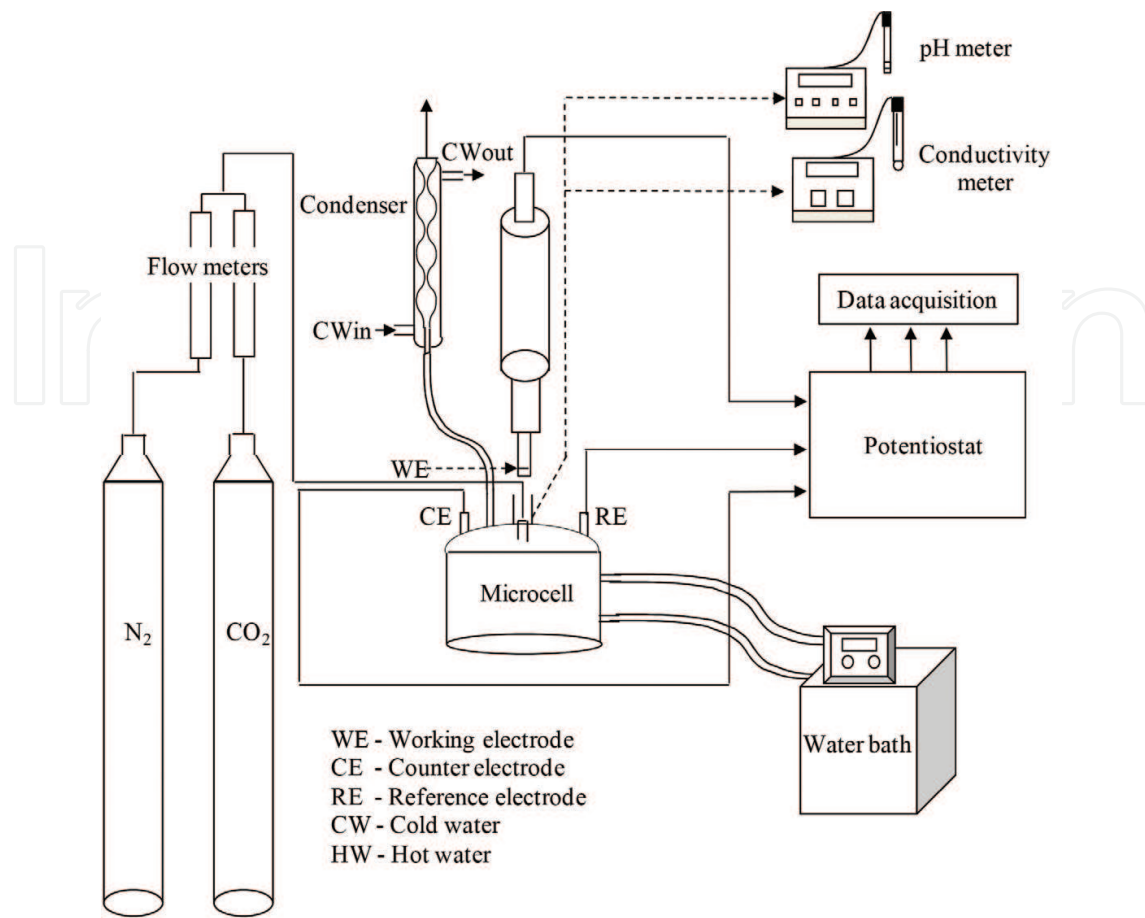
Figure 1. A schematic diagram of the electrochemical corrosion testing system.

results. A pH meter (Oakton pH 510 series) and a conductivity meter (YSI 3200 conductivity instrument) were connected to the setup for sample measurements.

3.2. Specimen preparation

Carbon steel (CS 1018) with the composition of 0.175% carbon, 0.75% manganese, and balance iron was chosen as the working electrode due to its common use as the construction material in amine-based CO_2 absorption plants [17]. The specimens were cylindrical with a dimension of 0.8 cm in height, 1.2 cm in diameter, and 0.6 cm central hole. Prior to each experiment, the specimens were surface finished with up to 600 grit silicon, degreased with methanol, rinsed with deionized water, and dried with air.

3.3. Solution preparation

A 5.0 kmol/m³ aqueous solution of monoethanolamine (MEA) was used as the CO_2 absorption solvent to simulate the service process solution [1]. The MEA solution was prepared from 99% reagent grade MEA and deionized water, purged with CO_2 to achieve a saturation loading of 0.55 ± 0.05 mol CO_2/mol MEA and added with a tested corrosion inhibitor. The inhibitor concentrations were in the range of 250–10,000 ppm. To evaluate the performance of the tested inhibitors in the MEA solution containing process contaminants, 10,000 ppm of the representative process contaminants, namely sodium chloride (NaCl) and formic acid

(CH_2O_2), were introduced to the MEA solution. A titration-based Chittick apparatus together with hydrochloric acid (HCL) and methyl orange indicators was used for analyzing MEA concentration and CO_2 loading.

3.4. Validation of experimental setup and procedure

Prior to tests, the anodic polarization and impedance scans of stainless steel (SS430) specimens were carried out in accordance with the ASTM G5-94 (reapproved in 2004) [18] and the ASTM G106-89 (reapproved in 2010) [19], respectively. The anodic polarization scan was done in a 1.0-N sulfuric acid (H_2SO_4) solution that was deaerated with nitrogen (N_2) at 30°C. The impedance scan was conducted using a deaerated 0.495-M sodium sulfate (Na_2SO_4) solution containing 0.005 M·H_2SO_4 at 30°C. The results of both scans were comparable to those of the ASTM standards, thus validating the experimental setup and the polarization and impedance procedures.

3.5. Experimental procedure

Prior to each test, the prepared MEA solution was transferred to a microcell where the solution temperature was controlled at 80°C, the CO_2 loading was maintained at saturation by CO_2 purging, and the solution concentration was kept at 5.0 kmol/m³. The open circuit potentials (OCP) were monitored with time until they reached equilibrium. The impedance scan was performed using 10 mV AC amplitude over a frequency range of 10 kHz–10 MHz. The corresponding impedance results were recorded in respect of frequency. After the impedance scan, the cyclic potentiodynamic polarization scan was then performed at 10 mV per minute. The solution samples were taken for the analysis of MEA concentration, CO_2 loading, pH, and conductivity before and after the electrochemical scans. The tested specimen was taken for surface analysis using the scanning electron microscopy (SEM).

3.6. Data analysis

The corrosion current density (i_{corr}) in the unit of µA/cm² was determined from the obtained potentiodynamic polarization data using the Tafel extrapolation. It was subsequently translated to corrosion rate (CR) in the unit of mmpy using the following equation:

$$CR = \frac{3.27 \times 10^{-3} \, a i_{corr}}{nD} \tag{1}$$

where a, n, and D represent atomic weight, number of electrons, and density of specimen in g/cm³, respectively. The obtained corrosion rates of the uninhibited and inhibited specimens were then used for determining the inhibition efficiency (IE).

$$IE = \left(\frac{CR_{uninhibited} - CR_{inhibited}}{CR_{uninhibited}} \right) \tag{2}$$

4. Results and discussion

The corrosion inhibition performance of seven selected compounds in aqueous solutions of MEA was evaluated under test conditions listed in **Table 4**. The evaluation was done in the

Parameter	Test condition
Amine type	Monoethanolamine (MEA)
Amine concentration (kmol/m³)	5.0 ± 0.1
Temperature (°C)	80.0 ± 1.0
CO$_2$ loading (mol CO$_2$/mol amine)	Saturation (0.55 ± 0.05)
Process contaminants	Chloride formate
Tested corrosion inhibitors	2-aminobenzene sulfonic acid
	3-aminobenzene sulfonic acid
	4-aminobenzene sulfonic acid
	Sulfapyridine
	Sulfanilamide
	Sulfolane
	Thiosalicylic acid
Inhibitor concentration (ppm)	
2-aminobenzene sulfonic acid	250, 500, 1000, 2000, 3000, 10,000
3-aminobenzene sulfonic acid	250, 500, 1000, 2000, 3000, 10,000
4-aminobenzene sulfonic acid	250, 500, 1000, 2000, 3000, 10,000
Sulfapyridine	500, 1000, 2000, 3000, 5000, 7000, 10,000
Sulfanilamide	3000, 10,000
Sulfolane	1000, 2000, 3000, 5000, 10,000
Thiosalicylic acid	3000, 10,000

Table 4. Summary of experimental parameters and conditions.

absence and presence of process contaminants (i.e., chloride and formate). Chloride was chosen because it is in the water used for the amine solution preparation and also found in the coal-fired flue gas fed to the carbon capture process. Formate was chosen because it is one of the predominant heat-stable salts produced from oxidative degradation of the amine solutions.

4.1. 2-aminobenzene sulfonic acid

4.1.1. Absence of process contaminants

The corrosion inhibition performance of 2-aminobenzene sulfonic acid was evaluated as a function of the inhibitor concentration. It is seen in **Figure 2a** that the corrosion rate of carbon steel in the 2-aminobenzene sulfonic acid-inhibited MEA solution significantly reduced from 4.27 mmpy (uninhibited) to 0.46–0.57 mmpy with inhibition efficiencies of 87–89%, when the inhibitor concentrations were in the range of 250–3000 ppm. However, at 10,000 ppm, the corrosion rate increased to 1.62 mmpy and the inhibition efficiency reduced to 62%.

From the potentiodynamic polarization curves in **Figure 2b**, it is apparent that, in the inhibited solutions, the carbon steel specimens were in an active state similar to the specimen in the uninhibited solution. The cathodic polarization curves shifted to lower current densities
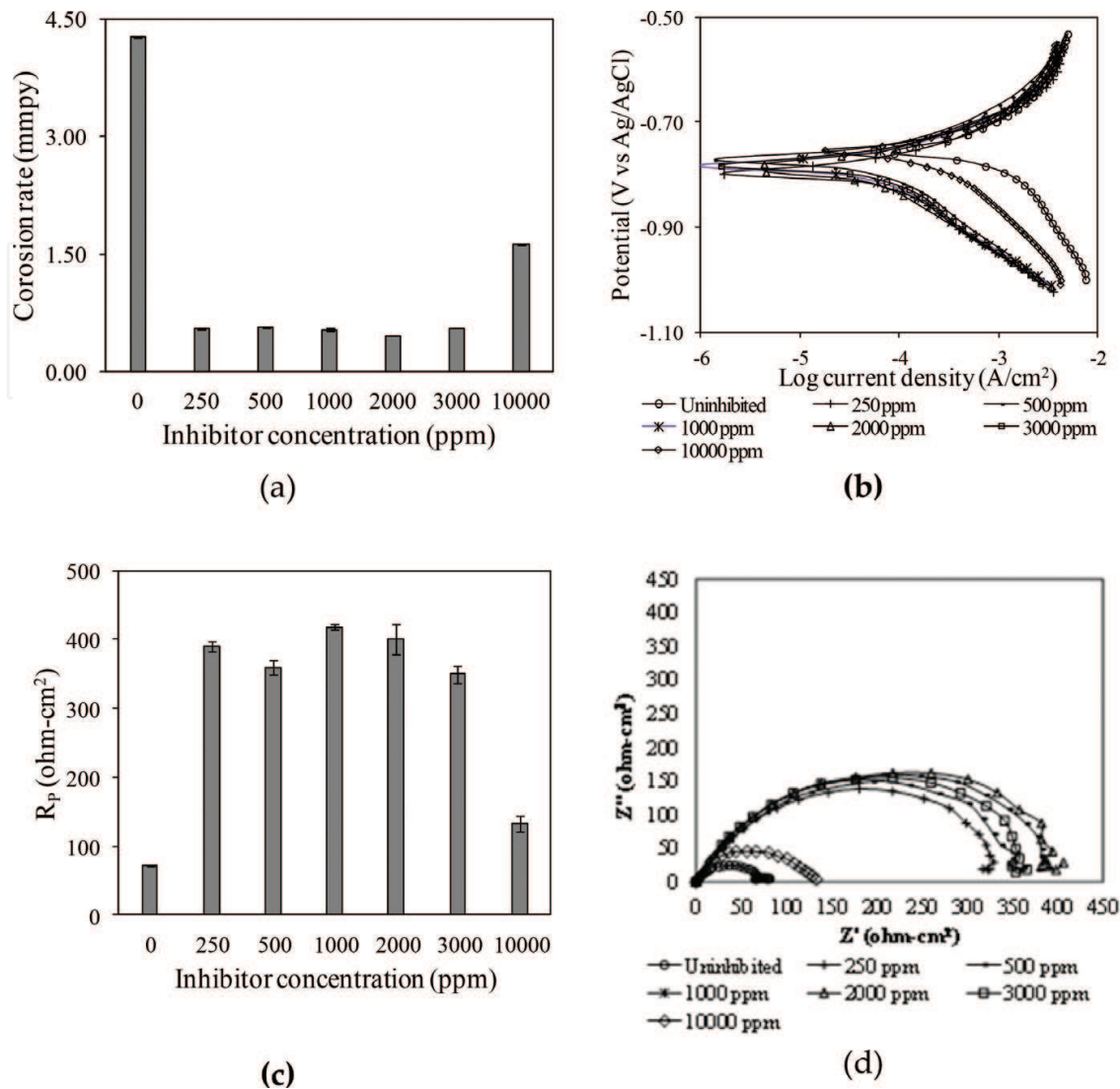
Figure 2. Corrosion inhibition performance of 2-aminobenzene sulfonic acid in 5.0 kmol/m^3 MEA solutions containing 0.55 mol/mol CO_2 loading in the absence of process contaminants at 80°C. (a) corrosion rate, (b) polarization curve, (c) polarization resistance, and (d) impedance behavior.

compared to the uninhibited condition while the anodic polarization curves remained unchanged. This suggests that the corrosion inhibition was cathodic in nature and was due to the preferential adsorption of inhibitor molecules onto the cathodic sites of the metal surface. The change in Tafel slopes of the inhibited potentiodynamic polarization curves compared to the uninhibited condition suggests a change in the corrosion mechanism. From the cyclic polarization curve obtained, no pitting was induced by the presence of 2-aminobenzene sulfonic acid at all tested concentrations.

The polarization resistance (R_p) values were analyzed from the obtained impedance data of the uninhibited and inhibited MEA solutions to reveal the effect of inhibitor concentration on inhibition performance. **Figure 2c** shows that the values of R_p increased from 72 (uninhibited) to 418 ohm-cm^2 when the concentration of 2-aminobenzene sulfonic acid was raised to 3000 ppm. However, the R_p value decreased to 134 ohm-cm^2 when the concentration of 2-aminobenzene sulfonic acid further increased to 10,000 ppm.

From **Figure 2d**, the Nyquist plots of inhibited solutions were in a semicircle shape representing a capacitive loop due to charge transfer kinetics. This suggests that the inhibitor protected the carbon steel surface by adsorption of inhibitor molecules, not by forming a passive barrier. The reduction in the inhibition performance at 10,000 ppm may have been caused by the lateral interactions of the adsorbed inhibitor on the metal surface [20].

4.1.2. Presence of process contaminants

Results in **Figure 3** show that chloride has a negligible effect on the inhibition performance of 2-aminobenzene sulfonic acid. The inhibited corrosion rate in the presence of chloride (i.e., 0.62 mmpy) was slightly higher than that with no process contaminants (i.e., 0.54 mmpy). This was confirmed by a small reduction in the R_p value from 418 to 380 ohm-cm^2 due to the presence of chloride. The inhibition efficiency was slightly reduced from 87 to 86%, which is considered negligible.

In contrast, formate appears to deteriorate the performance of 2-aminobenzene sulfonic acid. When 10,000 ppm formate was present in the solution, the inhibited corrosion rate increased from 0.54 to
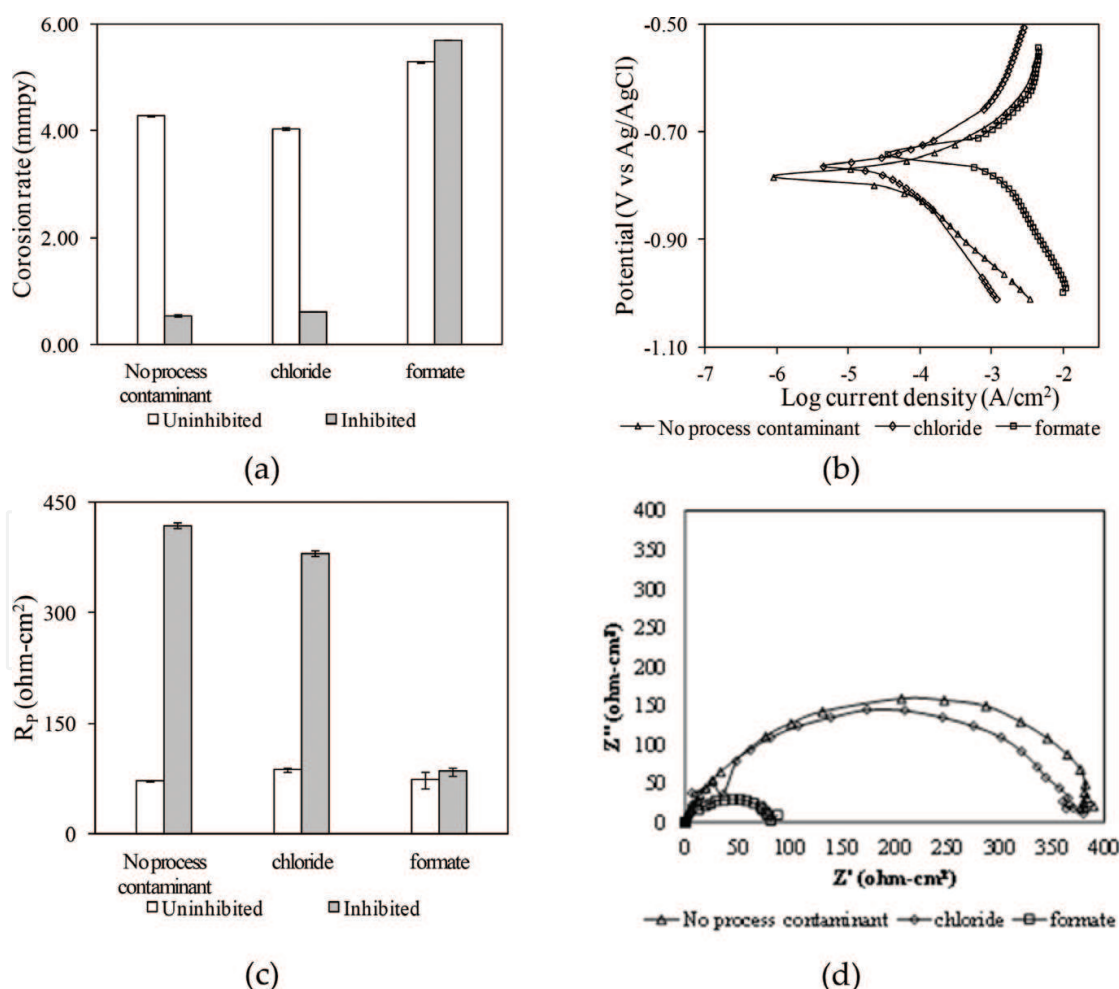

Figure 3. Corrosion inhibition performance of 1000 ppm of 2-aminobenzene sulfonic acid in 5.0 kmol/m^3 MEA solutions containing 0.55 mol/mol CO_2 loading in the presence of process contaminants at 80°C. (a) Corrosion rate, (b) polarization curve, (c) polarization resistance, and (d) impedance behavior.

5.70 mmpy with a significant reduction in the R_p value from 418 to 85 ohm-cm^2. Such an increase in the corrosion rate can also be observed by the significant shift of cathodic polarization curves to greater current densities. This suggests that the adsorption of inhibitor molecules on the metal surface may have been disrupted, thus allowing higher transport rate of corroding agents between the metal surface and the solution. No pitting was induced by the presence of chloride and formate.

4.2. 3-aminobenzene sulfonic acid

4.2.1. Absence of process contaminants

The 3-aminobenzene sulfonic acid performed well in the 5.0 kmol/m^3 MEA containing 0.55 mol/mol CO_2 loading and no process contaminants at 80°C. From **Figure 4**, the corrosion rates of carbon steel specimens were 0.48–0.49 mmpy with 89% inhibition efficiency when the concentrations of 3-aminobenzene sulfonic acid were in the range of 250–3000 ppm. This was confirmed by the R_p values that increased from 72 to 369–428 ohm-cm^2. Such a reduction in corrosion rates was a result of cathodic inhibition by 3-aminobenzene sulfonic acid. The cathodic polarization curves of the inhibited solutions shifted to lower current densities compared to that of the uninhibited. This suggests that this inhibitor acted as the cathodic inhibitor that impeded cathodic reactions by the adsorption of inhibitor molecules onto the metal surface. No pitting was observed from the cyclic polarization curves and surface analysis.

Results in **Figure 4** also show that applying this inhibitor at a high concentration of 10,000 ppm reduced the inhibition effectiveness. That is, the corrosion rate increased to 3.81 mmpy with the inhibition efficiency of 11% and the R_p of 88 ohm-cm^2. Such reduction in the inhibition performance was observed from the cathodic polarization curves of the inhibited solutions that shifted toward the cathodic curve of the uninhibited solution. Their current densities were slightly lower than the uninhibited curve. The shift of the cathodic curve in this direction illustrates deterioration of adsorption performance of the inhibitor which might be due to the increased lateral attractions in the adsorbed layer of inhibitor molecules on the metal surface.

4.2.2. Presence of process contaminants

The presence of chloride and formate caused a negative effect on corrosion inhibition performance of 3-aminobenzene sulfonic acid. In **Figure 5** the corrosion rate in the inhibited solution containing chloride increased from 0.48 mmpy (in the absence of process contaminants) to 1.65 mmpy. As a result, the inhibition efficiency was reduced from 89 to 61%. In case of formate, the corrosion rate in the inhibited solution increased to 5.31 mmpy, thus reducing the inhibition efficiency to −24%. This indicates that the inhibitor did not retard the corrosion but in fact aggravated corrosion. The impedance results also support such behavior. That is, the R_p value decreased from 369 ohm-cm^2 (in the absence of process contaminants) to 88 ohm-cm^2 in the presence of chloride and to 105 ohm-cm^2 in the presence of formate.

The deterioration of inhibition performance in the presence of chloride and formate can be observed from the potentiodynamic polarization curves. The tested carbon steel underwent active corrosion, and the cathodic current densities were greater in the presence of contaminants than those in the absence of contaminants. This might be due to the disruption of the adsorption of 3-aminobenzene sulfonic acid molecules onto the metal surface in the presence of process contaminants. The effect was more pronounced in the presence of formate than chloride.
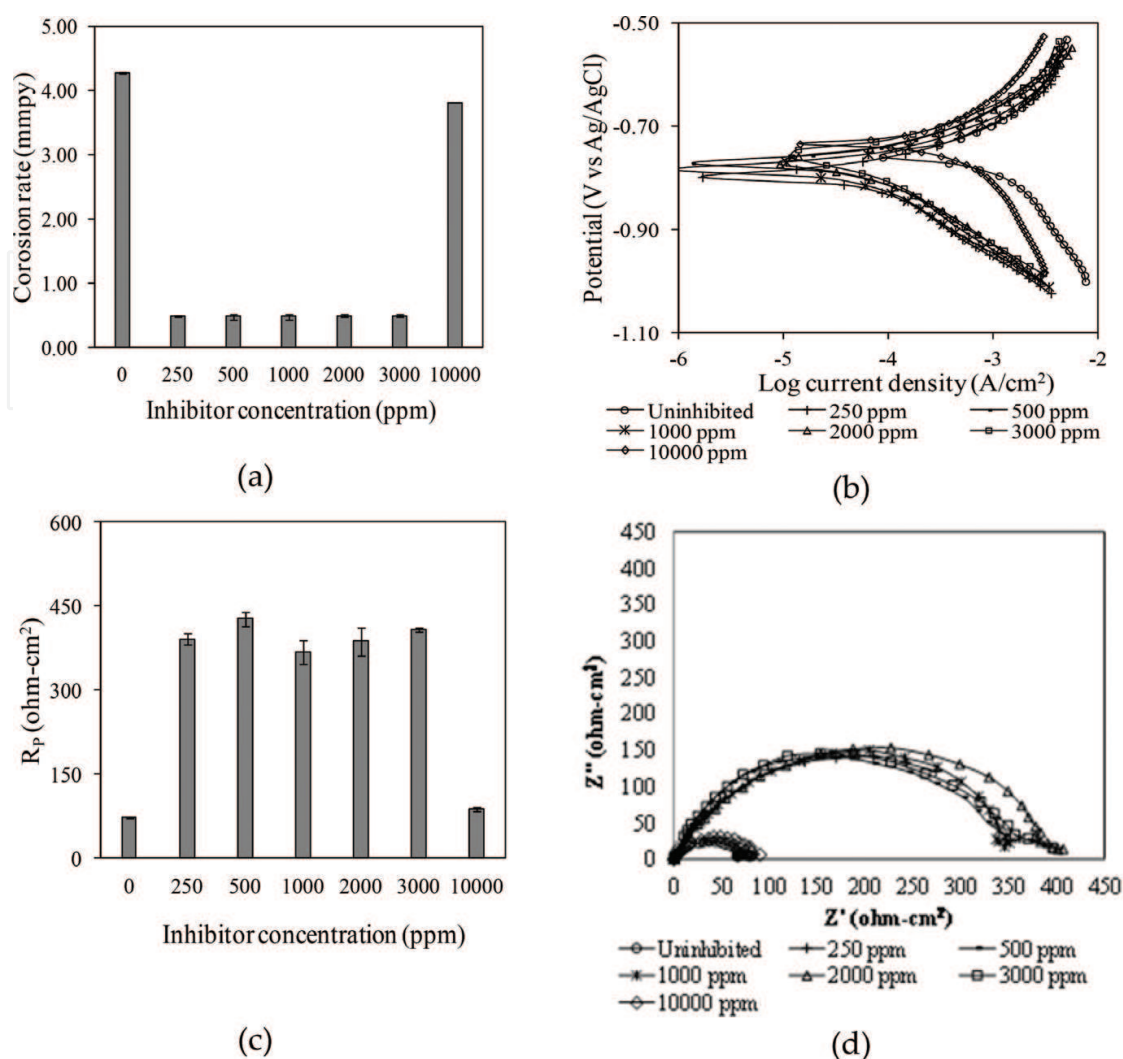
Figure 4. Corrosion inhibition performance of 3-aminobenzene sulfonic acid in 5.0 kmol/m^3 MEA solutions containing 0.55 mol/mol CO_2 loading in the absence of process contaminants at 80°C. (a) Corrosion rate, (b) polarization curve, (c) polarization resistance, and (d) impedance behavior.

It should be noted that the presence of chloride caused pitting corrosion on carbon steel in the MEA solution inhibited by 3-aminobenzene sulfonic acid. Pits were detected from the cyclic polarization curve in **Figure 6a** in the form of positive hysteresis, that is, the reverse curve lies to the right of the forward curve. These pits were also seen in an SEM image of the specimen after test (**Figure 6b**).

4.3. 4-aminobenzene sulfonic acid

4.3.1. Absence of process contaminants

4-Aminobenzene sulfonic acid significantly reduced the corrosion rates of carbon steel in the 5.0 kmol/m^3 MEA containing 0.55 mol/mol CO_2 loading and no process contaminant at 80°C. As shown in **Figure 7a**, the corrosion rate decreased from 4.27 to 0.38–0.56 mmpy with inhibition efficiencies of 87–91% when the inhibitor concentrations were in the range of 250–3000 ppm. However, the corrosion rate increased to 3.77 mmpy and the inhibition efficiency dropped to 12% when 10,000 ppm was used.
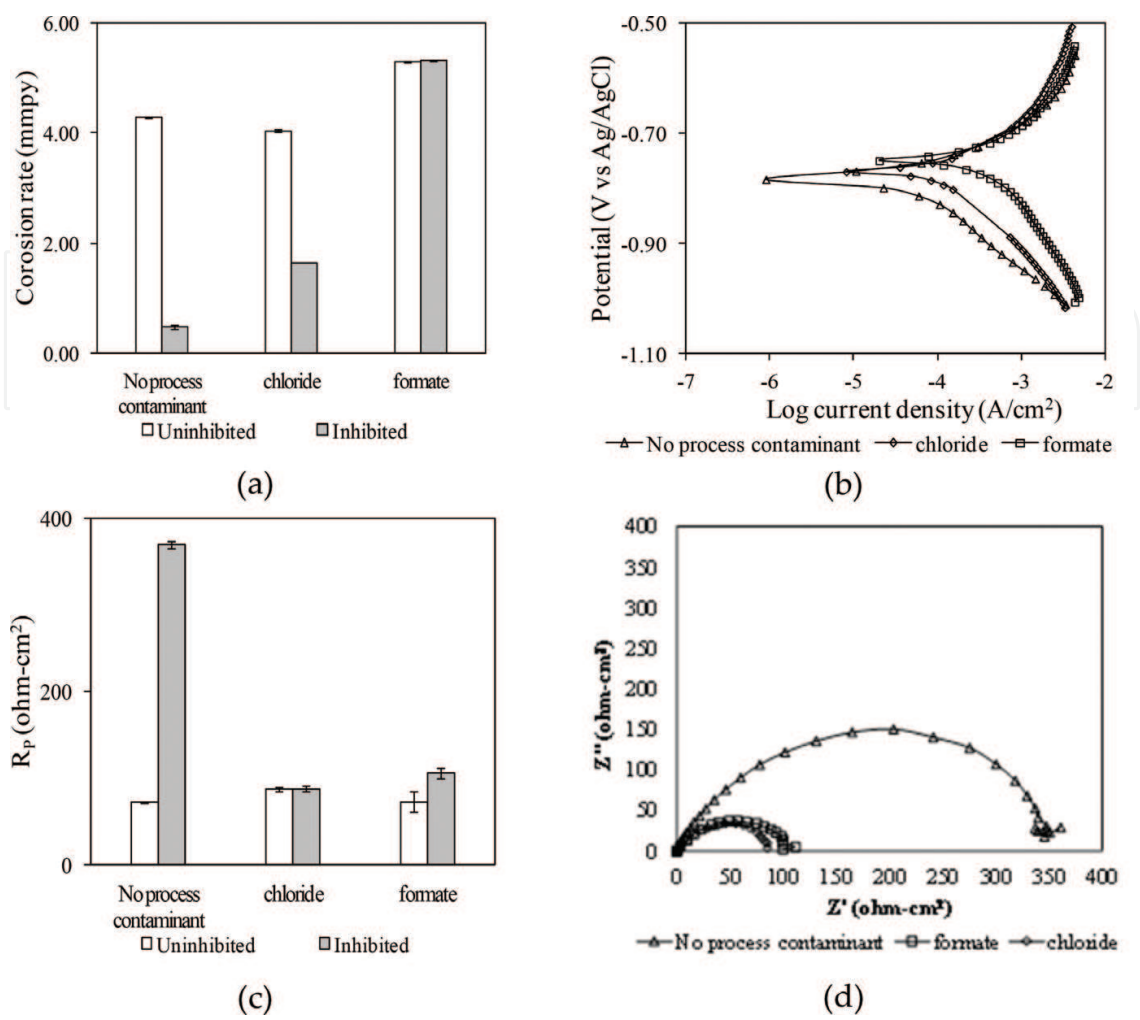
Figure 5. The corrosion inhibition performance of 1000 ppm of 3-aminobenzene sulfonic acid in 5.0 kmol/m³ MEA solutions containing 0.55 mol/mol CO_2 loading in the presence of process contaminants at 80°C. (a) Corrosion rate, (b) polarization curve, (c) polarization resistance, and (d) impedance behavior.
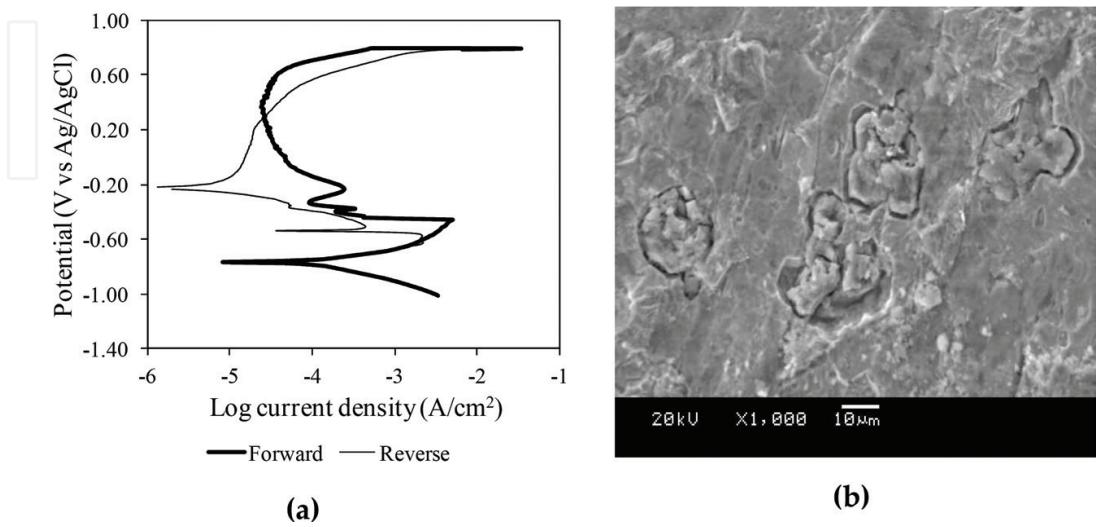

Figure 6. Pitting corrosion in 5.0 kmol/m³ MEA solutions containing 0.55 mol/mol CO_2 loading, inhibited by 1000 ppm of 3-aminobenzene sulfonic acid in the presence of 10,000 ppm chloride at 80°C (a) cyclic polarization curve showing positive hysteresis (b) SEM image showing pits with 1000× magnification.

Such inhibition performance of 4-aminobenzene sulfonic acid was observed by the potentio-dynamic polarization curves in **Figure 7b**. The tested specimens were in an active state. The 4-aminobenzene sulfonic acid functioned as a cathodic corrosion inhibitor. At 250–3000 ppm, the cathodic current densities were lower than the uninhibited cathodic current densities suggesting that the cathodic reactions were impeded by the adsorption of the tested inhibitor. No pitting tendency was induced by the presence of 4-aminobenzene sulfonic acid at any concentrations.

The values of R_p obtained from impedance analysis (**Figure 7c**) showed similar results to the polarization analysis. The R_p was in the range of 355–460 ohm-cm^2 at the inhibitor concentrations of 250–3000 ppm and then dropped to 99 ohm-cm^2 at the inhibitor concentration of 10,000 ppm. The impedance analysis (**Figure 7d**) yielded a semicircle characteristic of charge transfer kinetics at the metal-solution interface, suggesting that no passive layer was present.

4.3.2. Presence of process contaminants

The corrosion inhibition performance of 4-aminobenzene sulfonic acid at 1000 ppm was unaffected by the presence of chloride but deteriorated in the presence of formate. No pitting tendency was found in either case. From **Figure 8a**, the corrosion rate of a carbon steel specimen remained close to the uncontaminated corrosion rate (0.45 mmpy) when 10,000 ppm chloride was added to the inhibited MEA solution. The presence of chloride did not alter anodic and cathodic polarization behavior of the inhibited MEA solution. On the contrary, the addition of 10,000 ppm formate into the inhibited MEA solution aggravated corrosion and caused the corrosion rate of the inhibited MEA solution to increase to 5.45 mmpy (−28% inhibition efficiency) which exceeded the corrosion rate of the uninhibited solution. This effect was evidenced by the shift of the cathodic polarization curve to higher current densities in **Figure 8b**. Such a shift of the cathodic curve implied a higher flux of corroding agents on the metal surface, which resulted from the deficiency of adsorption of inhibitor molecules onto the metal surface in the presence of formate.

The impedance results (**Figure 8c**) also confirm the abovementioned findings. The R_p in the presence of chloride (385 ohm-cm^2) was slightly lower than the no contaminant condition (441 ohm-cm^2) whereas the R_p in the presence of formate (87 ohm-cm^2) was drastically lower. A semicircular loop in **Figure 8d** exhibited charge transfer kinetics.

4.4. Sulfapyridine

4.4.1. Absence of process contaminants

From **Figure 9a**, it was apparent that sulfapyridine was not effective at 500 and 1000 ppm in the 5.0 kmol/m^3 MEA containing 0.55 mol/mol CO_2 loading and no process contaminant at 80°C. At 500 ppm, the corrosion rate of carbon steel remained at 4.27 mmpy which was the corrosion rate of the uninhibited solution. At 1000 ppm, the corrosion rate was reduced to 3.07 mmpy with an inhibition efficiency of 28%. The inhibition efficiency was significantly increased to 90–92% with a reduction in corrosion rates to 0.33–0.44 mmpy when sulfapyridine concentration increased to the range of 2000–10,000 ppm.

The effectiveness of sulfapyridine can be observed from potentiodynamic polarization curves in **Figure 9b**. The addition of sulfapyridine caused the cathodic polarization curves to shift to
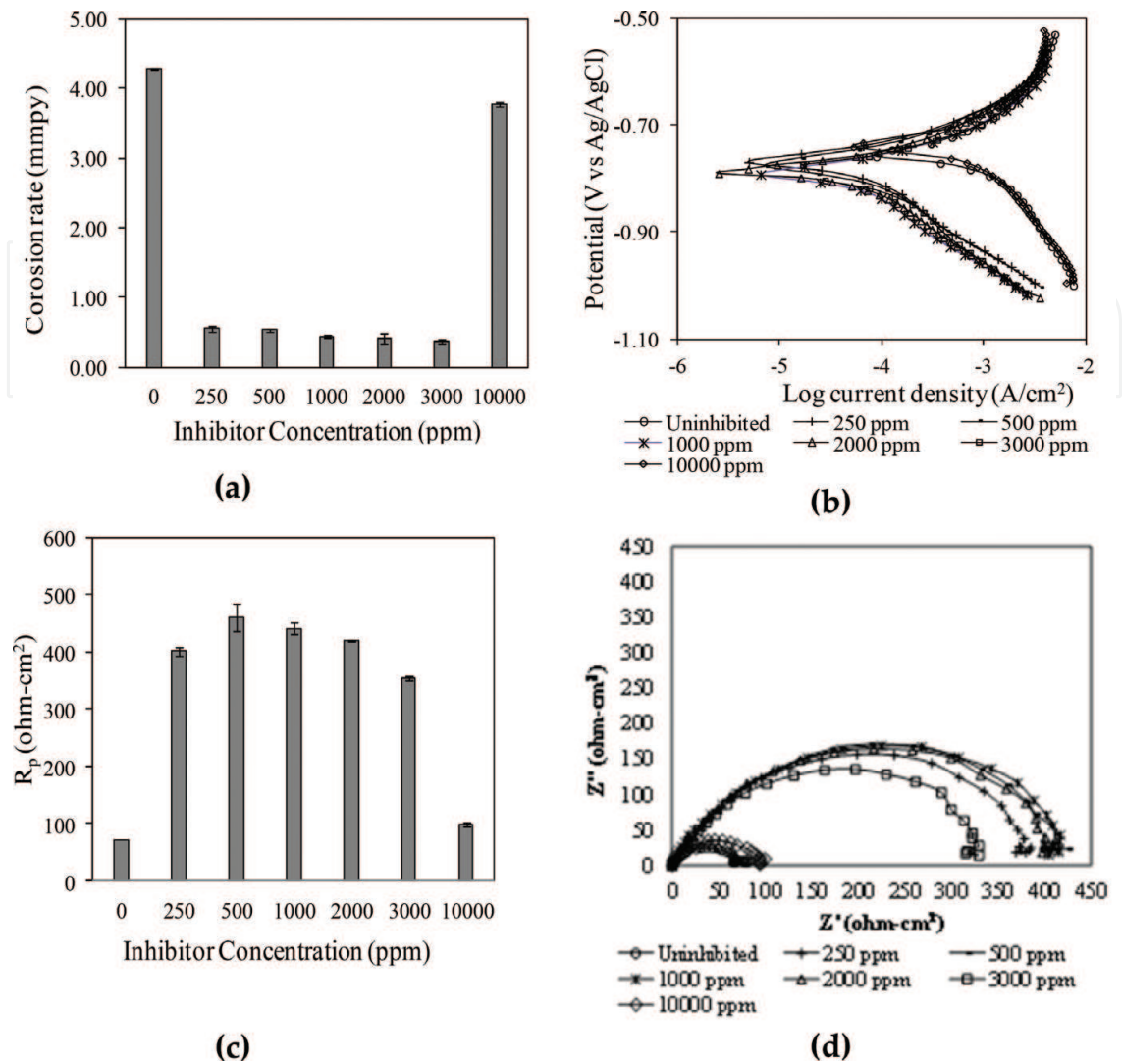
Figure 7. The corrosion inhibition performance of 4-aminobenzene sulfonic acid in 5.0 kmol/m^3 MEA solutions containing 0.55 mol/mol CO_2 loading in the absence of process contaminants at 80°C. (a) Corrosion rate, (b) polarization curve, (c) polarization resistance, and (d) impedance behavior.

lower current densities but did not alter the anodic curves. This suggested that sulfapyridine acted as a cathodic inhibitor which formed an adsorption layer onto the metal-solution inter-face and thus retarded the mass transfer rate of corroding agents. The cyclic polarization curves and the surface analysis revealed no pitting corrosion at any concentrations of sulfapyridine.

The R_p obtained from the impedance analysis (**Figure 9c**) reinforced the above findings in that sulfapyridine did not function effectively below 2000 ppm. The R_p value of the MEA solution containing 500 ppm sulfapyridine was 86 ohm-cm^2, which was similar to the R_p of the unin-hibited solution. However, once the sulfapyridine concentration increased to 1000 ppm, the R_p value began to rise to 105 ohm-cm^2. The R_p was further increased to 397–528 ohm-cm^2 when the sulfapyridine concentrations were 2000–10,000 ppm. The impedance analysis (**Figure 9d**) also showed the semicircular loop characteristic of charge transfer kinetics at the interface, suggesting the absence of passive layer. Hence, the higher R_p values obtained were due to the adsorption of sulfapyridine onto the metal surface.
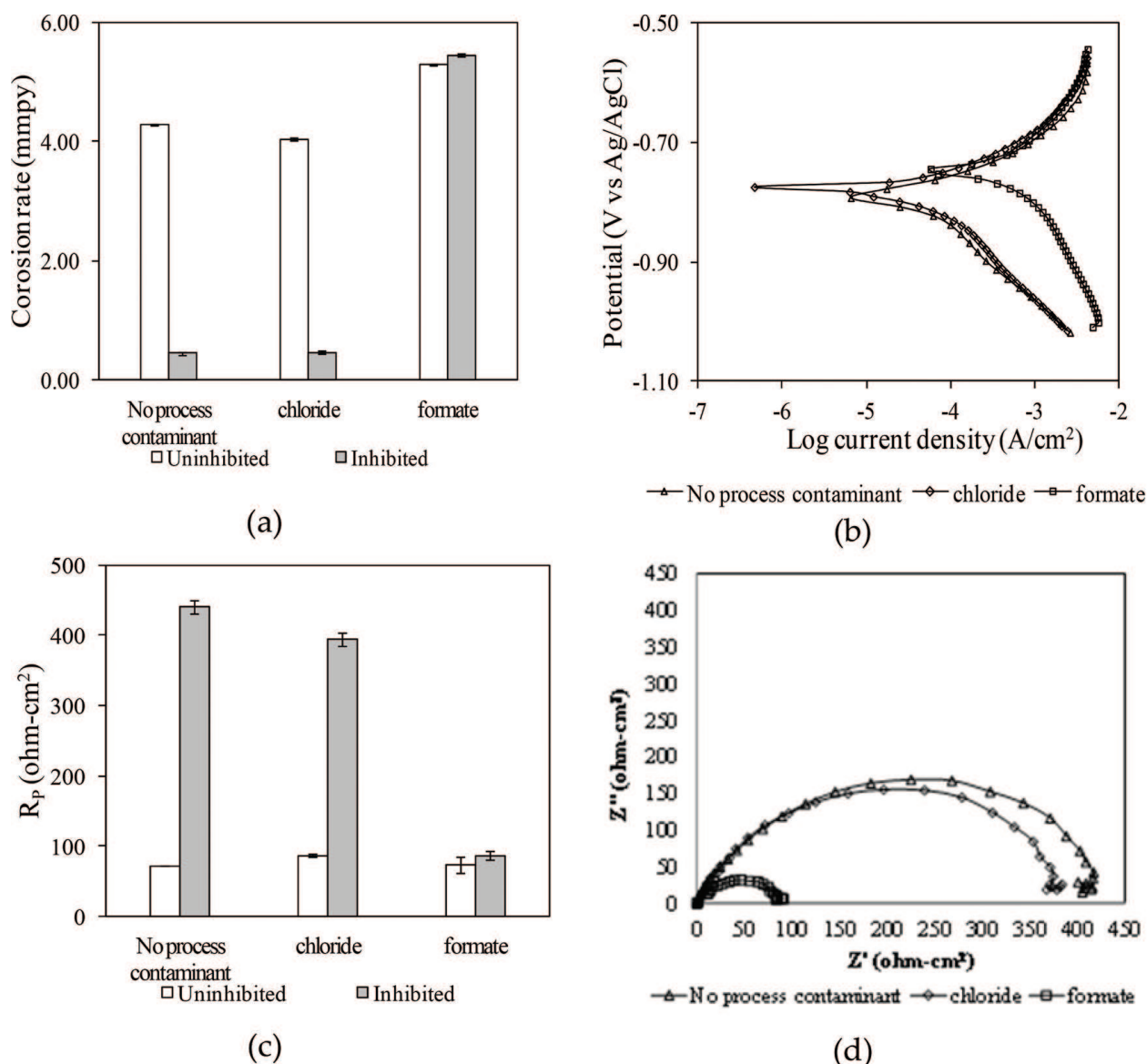
Figure 8. Corrosion inhibition performance of 1000 ppm of 4-aminobenzene sulfonic acid in 5.0 kmol/m³ MEA solutions containing 0.55 mol/mol CO_2 loading in the presence of process contaminants at 80°C. (a) Corrosion rate, (b) polarization curve, (c) polarization resistance, and (d) impedance behavior.

4.4.2. Presence of process contaminants

Figure 10 shows that the presence of formate in the MEA solution did not have an apparent effect on the inhibition performance of sulfapyridine. When 10,000 ppm formate was present in the MEA solution, the inhibition efficiency of sulfapyridine slightly reduced from 90% (in the absence of formate) to 88%, and the R_p value also reduced from 468 to 358 ohm-cm². This result can also be observed from a slight shift of the cathodic polarization curve to lower current densities.

Unlike formate, chloride had a detrimental effect on the inhibition performance of sulfapyridine. The presence of 10,000 ppm chloride in the MEA solution caused the corrosion rate of carbon steel to increase from 0.44 mmpy (in the sulfapyridine-inhibited MEA solution) to 4.34 mmpy, reflecting a reduction of the inhibition performance from 90% to −2%. The R_p value was significantly
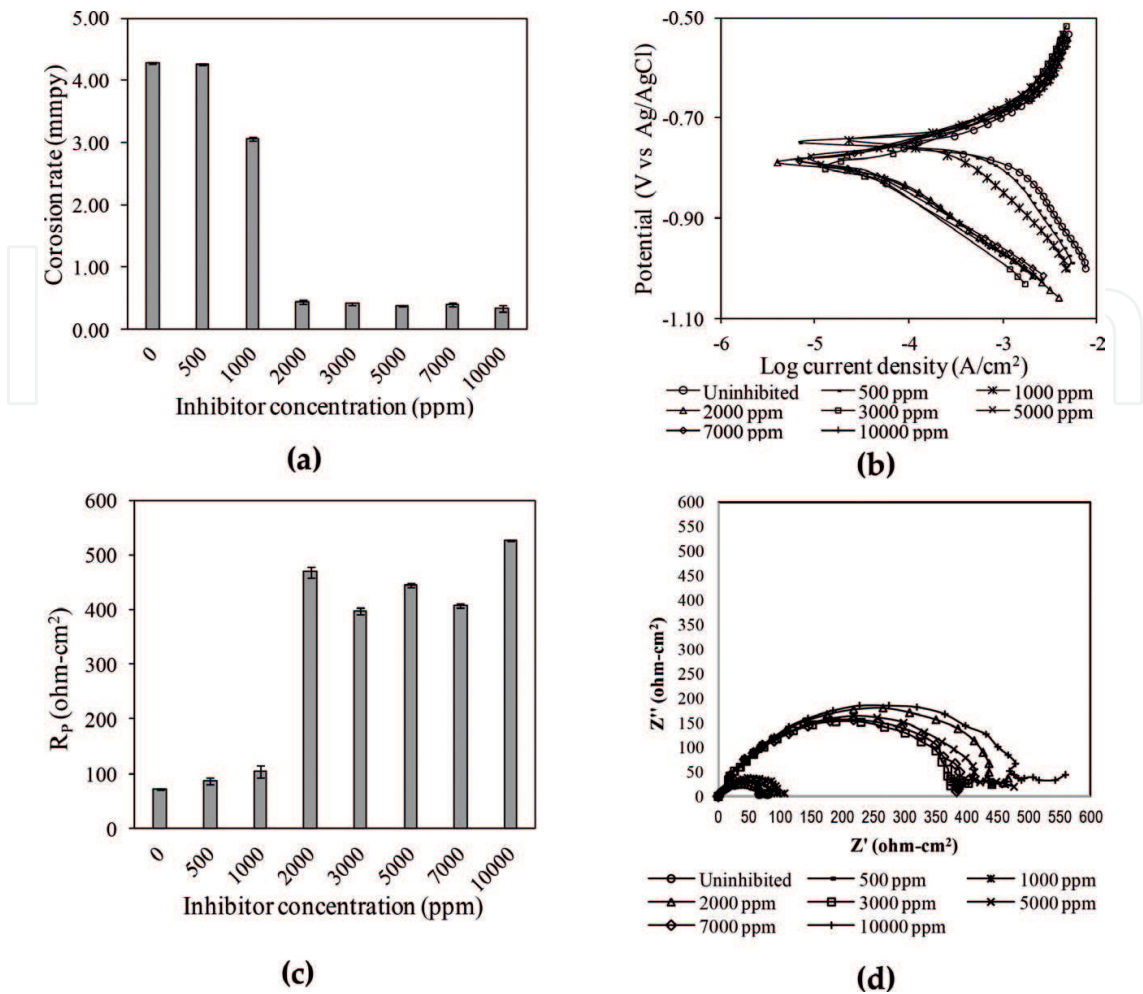
Figure 9. Corrosion inhibition performance of sulfapyridine in 5.0 kmol/m³ MEA solutions containing 0.55 mol/mol CO_2 loading in the absence of process contaminants at 80°C. (a) Corrosion rate, (b) polarization curve, (c) polarization resistance, and (d) impedance behavior.

reduced from 468 to 91 ohm-cm², which is close to the R_p of the uninhibited MEA solution. The cathodic polarization curve of the sulfapyridine MEA solution shifted to much higher current densities in the presence of chloride. This suggested that chloride could destroy the inhibition adsorption ability of sulfapyridine. No pitting was induced in the presence of both formate and chloride.

4.5. Sulfanilamide

Sulfanilamide did not perform well in the 5.0 kmol/m³ MEA solution containing 0.55 mol/mol CO_2 loading at 80°C. When 3000 and 10,000 ppm sulfanilamide were introduced to the MEA solutions, the corrosion rate of carbon steel reduced from 4.27 mmpy to 2.50 and 3.41 mmpy, respectively, with corresponding inhibition efficiencies of 42 and 20% (**Figure 11a**). Such poor inhibition performance of sulfanilamide was apparent from small shifts of cathodic curves from the uninhibited curve (**Figure 11b**) and small increments of R_p in the presence of sulfanilamide (**Figure 11c**). The R_p increased from 72 ohm-cm² in the uninhibited MEA solution to only 104 and 84 ohm-cm² at 3000 and 10,000 ppm sulfanilamide, respectively. This reflected poor resistance of the adsorption layer on metal surface to the transport of corroding agents.
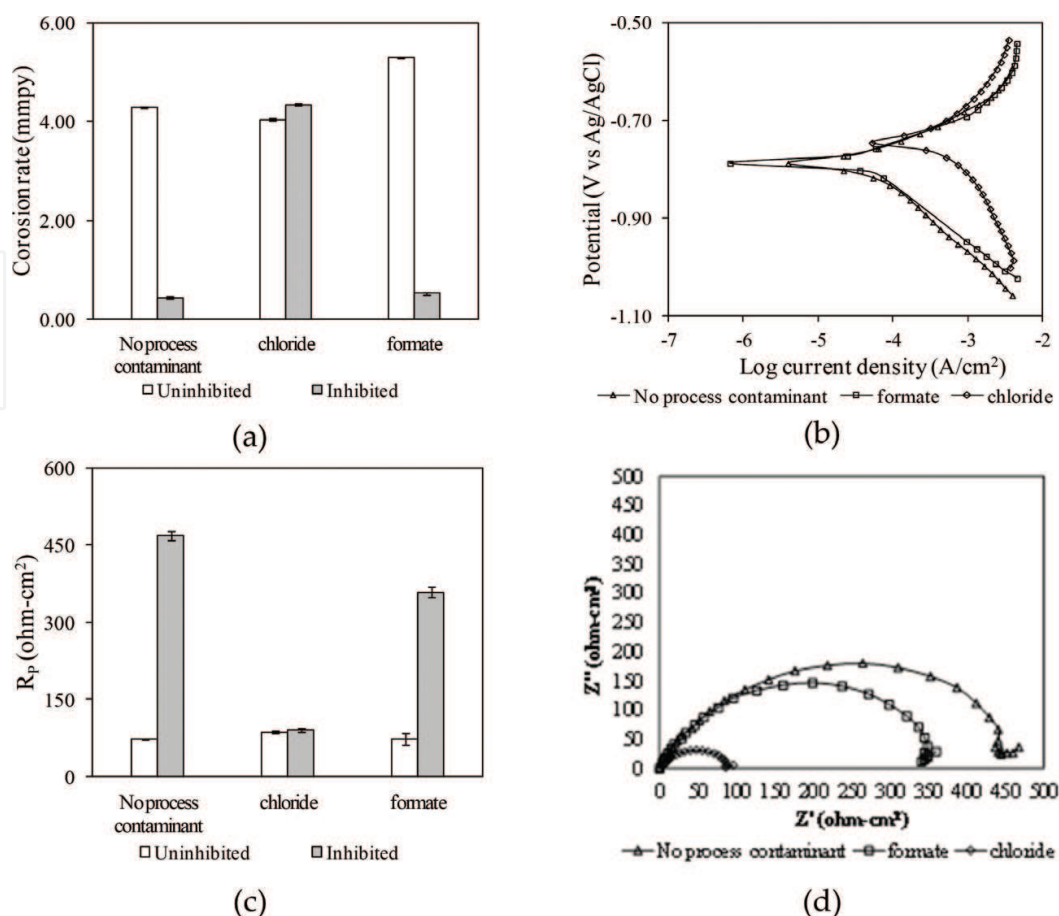
Figure 10. The corrosion inhibition performance of 2000 ppm of sulfapyridine in 5.0 kmol/m³ MEA solutions containing 0.55 mol/mol CO_2 loading in the presence of process contaminants at 80°C. (a) Corrosion rate, (b) polarization curve, (c) polarization resistance, and (d) impedance behavior.

The cyclic polarization curve and surface analysis showed no pitting in the presence of sulfanilamide at any concentrations. The impedance analysis (**Figure 11d**) traced a semicircle or a capacitive loop due to charge transfer kinetics similar to that of the uninhibited system, suggesting that no passive film developed on the surface. Since its corrosion inhibition efficiencies were much lower than other tested compounds, sulfanilamide was not further tested for the effect of process contaminants.

4.6. Sulfolane

4.6.1. Absence of process contaminants

Sulfolane was an effective corrosion inhibitor when an adequate concentration was introduced to the solution. As seen in **Figure 12a**, an addition of 1000 ppm sulfolane reduced the corrosion rate of carbon steel from 4.27 mmpy in the uninhibited solution to 3.63 mmpy with 15% inhibition efficiency. Once the concentration of sulfolane increased to 2000–10,000 ppm, the corrosion rate substantially reduced to 0.43–0.62 mmpy, with an inhibition efficiency of 85–90%. This finding was supported by the impedance analysis results (**Figure 12c** and **d**). The R_p increased from 116 to the range of 331–445 ohm-cm² when the concentration of sulfolane increased from 1000 to 2000–10,000 ppm. No pitting was induced by the presence of sulfolane at any concentrations.
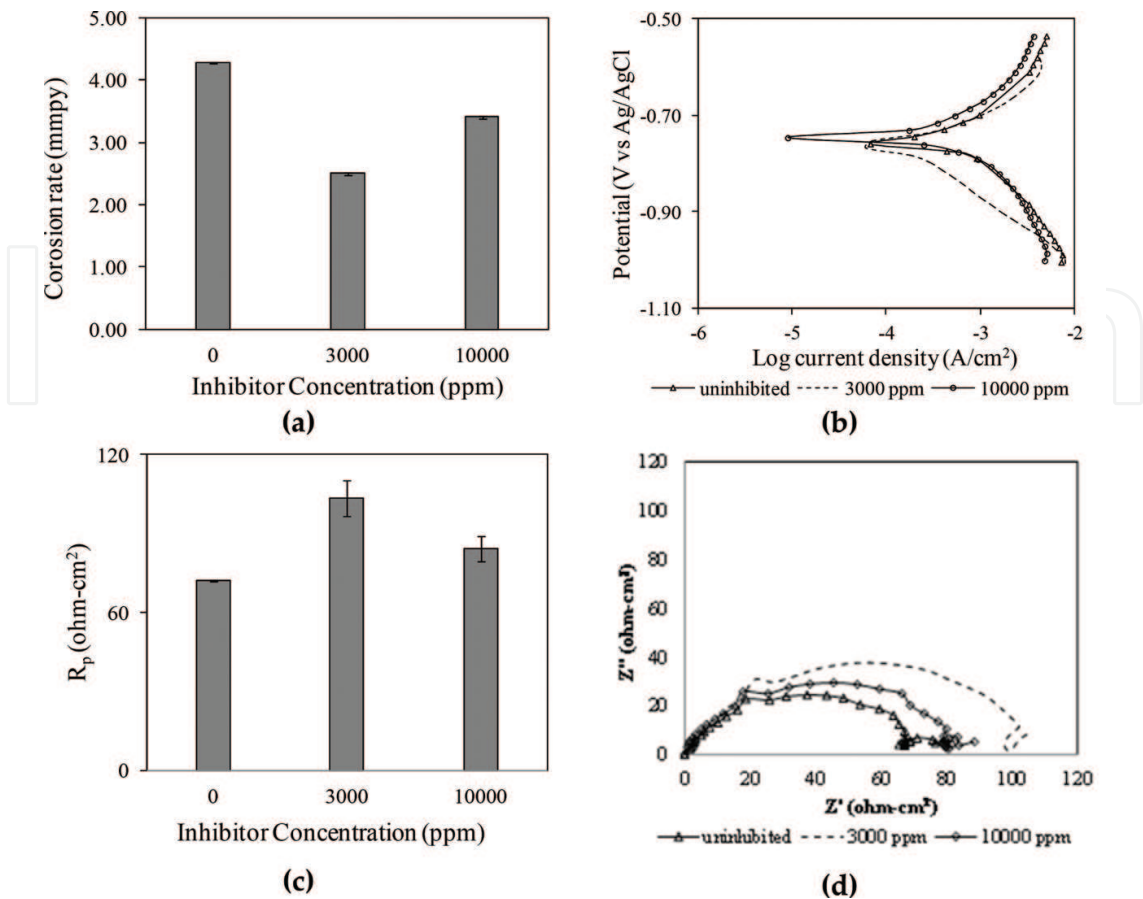
Figure 11. The corrosion inhibition performance of sulfanilamide in 5.0 kmol/m³ MEA solutions containing 0.55 mol/mol CO_2 loading in the absence of process contaminants at 80°C. (a) Corrosion rate, (b) polarization curve, (c) polarization resistance, and (d) impedance behavior.

The effectiveness of sulfolane can be explained by considering its polarization behavior in **Figure 12b**. The presence of sulfolane in the solution caused the cathodic polarization curve to shift to the direction of lower current densities but did not alter the anodic curve. This suggested that sulfolane acted as a cathodic inhibitor which was adsorbed onto the metal surface to inhibit the transport of corroding species between the metal surface and MEA solution. As a result, the rate of the cathodic reaction was retarded which was exhibited by the shift of the cathodic curve.

Due to the nature of inhibitor adsorption onto the metal surface, it is important to have sufficient inhibitor coverage on the metal surface. This was why the increasing sulfolane concentration from 1000 to 2000 ppm resulted in a much higher inhibition efficiency. However, an addition of a higher sulfolane concentration than 2000 ppm yields very small increases in efficiency. This suggested that the minimum concentration required for effective corrosion inhibition was 2000 ppm.

4.6.2. Presence of process contaminants

The inhibition performance of sulfolane was not considerably affected by the presence of chloride or formate. As illustrated in **Figure 13a**, the corrosion rate of carbon steel in the
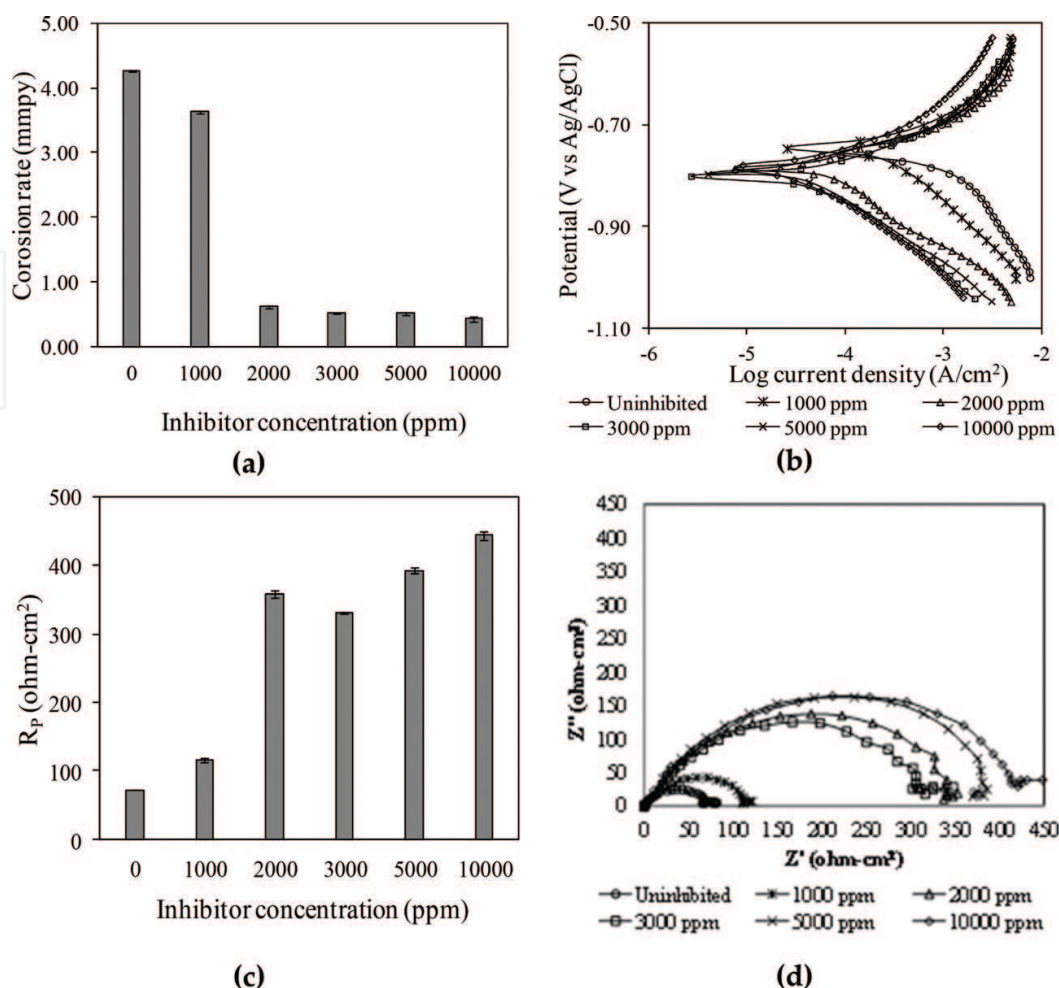
Figure 12. The corrosion inhibition performance of sulfolane in 5.0 kmol/m³ MEA solutions containing 0.55 mol/mol CO_2 loading in the absence of process contaminants at 80°C. (a) Corrosion rate, (b) polarization curve, (c) polarization resistance, and (d) impedance behavior.

sulfolane-inhibited solution did not change much when chloride or formate was added to the solution. The corrosion rates in the presence of chloride and formate were 0.48 and 0.44 mmpy, respectively, which were slightly lower than the corrosion rate in the absence of these two contaminants (0.62 mmpy). This reflects slight increases in inhibition efficiencies from 85% (the absence of contaminants) to 89–90% (the presence of formate and chloride). The insignificant effects of chloride and formate were also observed from the cathodic polarization curves (**Figure 13b**) that were not shifted from the no contaminant condition in the presence of chloride and formate. No pitting was induced by these two contaminants.

From the impedance analysis (**Figure 13c** and **d**), the R_p of formate-MEA-sulfolane solution (431 ohm-cm²) was higher than that of the MEA-sulfolane solution (358 ohm-cm²). This showed a small increase in the resistance developed on the metal surface in the presence of formate, which supported the above findings from the potentiodynamic polarization tests. However, the R_p of the chloride-containing solution decreased to 314 ohm-cm², which indicated a slight reduction in inhibition efficiency in the presence of chloride. Thus, this implied that chloride may slightly deteriorate the inhibition performance of sulfolane.
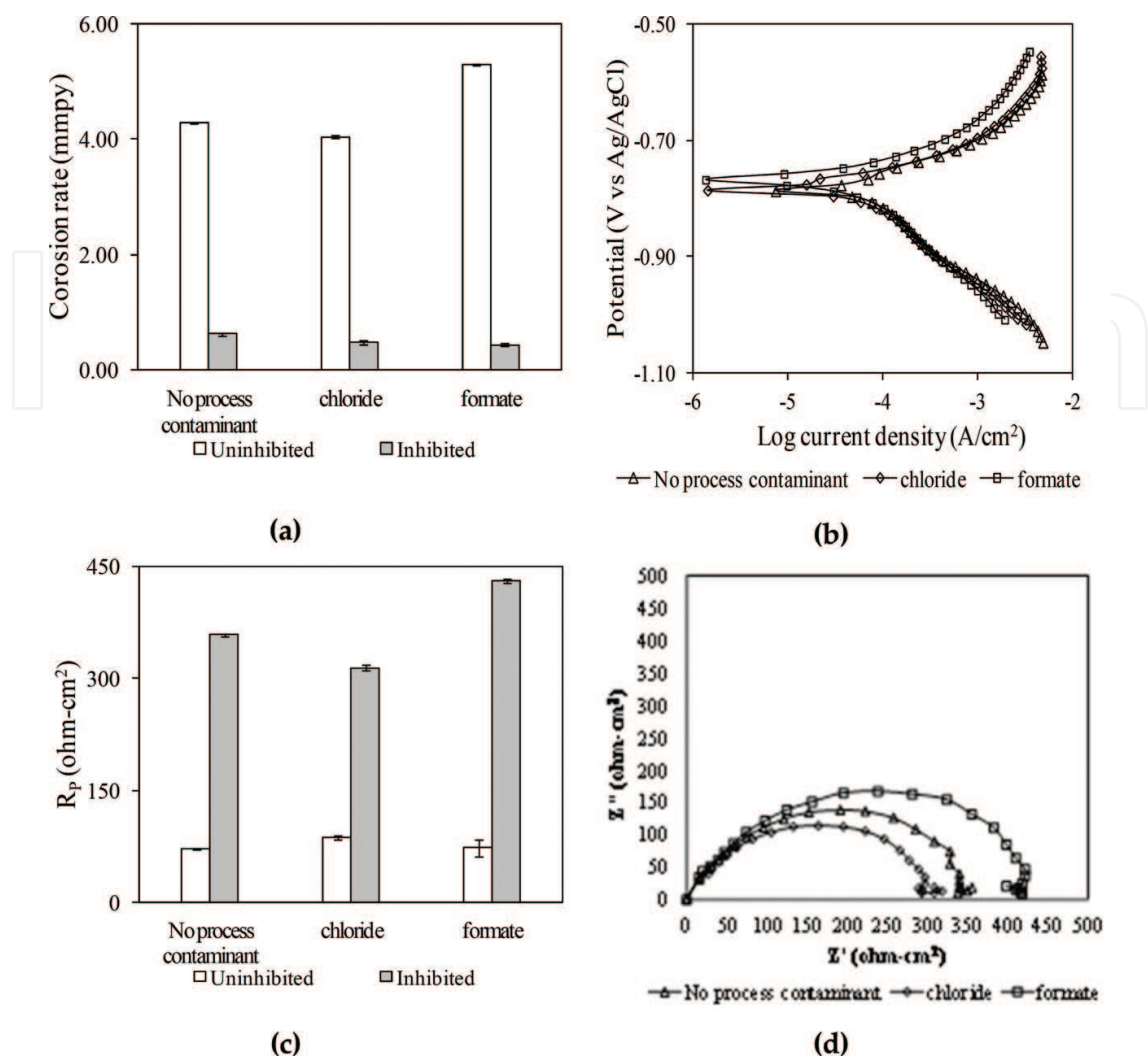
Figure 13. The corrosion inhibition performance of 2000 ppm of sulfolane in 5.0 kmol/m³ MEA solutions containing 0.55 mol/mol CO_2 loading in the presence of process contaminants at 80°C. (a) Corrosion rate, (b) polarization curve, (c) polarization resistance, and (d) impedance behavior.

4.7. Thiosalicylic acid

Thiosalicylic acid was found to reduce the corrosion rate of carbon steel from 4.27 mmpy in the uninhibited MEA solution to 0.84 and 2.24 mmpy with the inhibition efficiencies of 80 and 47% when its concentrations were 3000 and 10,000 ppm, respectively (**Figure 14a**). This finding was confirmed by the values of R_p from the impedance analysis (**Figure 14c**). That is, the R_p increased from 72 in the uninhibited MEA solution to 190 and 101 ohm-cm² for 3000 and 10,000 ppm thiosalicylic acid, respectively.

Similar to other tested inhibitors, thiosalicylic acid acted as a cathodic inhibitor. As shown in **Figure 14b**, an addition of thiosalicylic acid caused the cathodic curve to shift to lower current densities but did not shift the anodic curve. This indicated a resistance to the transportation of corroding species developed onto the metal surface. Such findings were also supported by
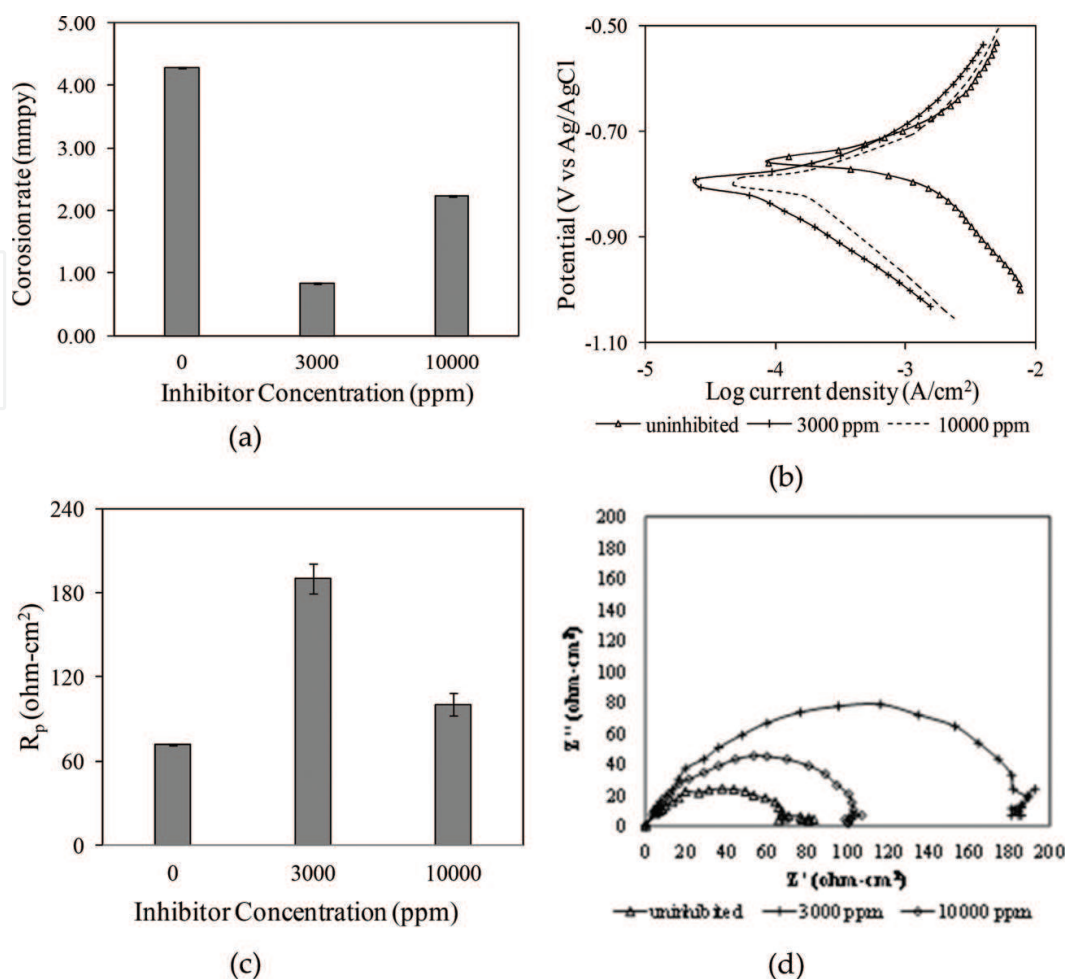
Figure 14. The corrosion inhibition performance of thiosalicylic acid in 5.0 kmol/m³ MEA solutions containing 0.55 mol/mol CO_2 loading in the absence of process contaminants at 80°C. (a) Corrosion rate, (b) polarization curve, (c) polarization resistance, and (d) impedance behavior.

the semicircle characteristic of a capacitive loop due to charge transfer kinetics at the interface in **Figure 14d**.

It should be noted that, in the course of the experiment, the test solutions containing thiosalicylic acid turned black at both 3000 and 10,000 ppm. This might be due to the incompatibility of the inhibitor with the MEA solution. Thus, thiosalicylic acid was not tested further at other concentrations and not tested for the effect of process contaminant.

4.8. Surface analysis

For the uninhibited MEA solution, a uniform corrosion product was formed over the metal surface as seen from the scanning electron microscopy (SEM) images in **Figure 15a**. A significant increase in the amounts of oxygen and carbon in the tested specimens was found in the energy-dispersive X-ray spectroscopy (EDS) analysis (**Figure 15b**) compared to the uncorroded specimens (**Figure 15d**). The peaks obtained from X-ray diffraction (XRD) analysis
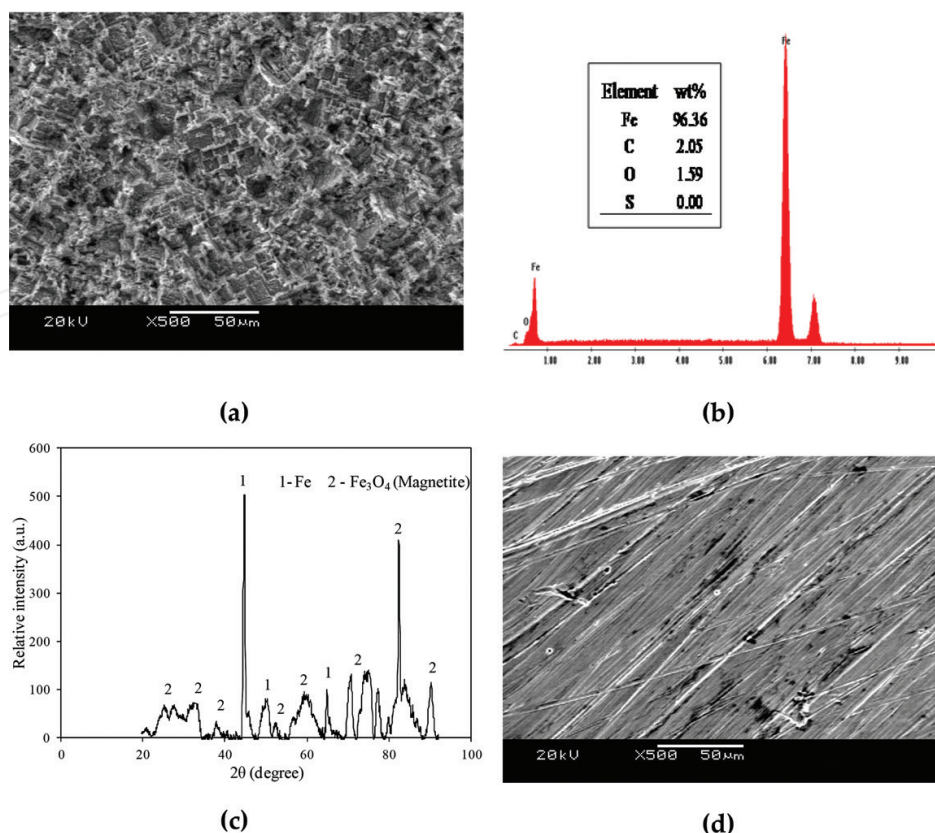
Figure 15. Surface analysis of CS 1018 in uninhibited 5.0 kmol/m³ MEA solutions at 80°C and 0.55 mol/mol CO$_2$ loading. (a) An SEM image of corroded specimen (500× magnification) after 28 days, (b) EDS spectra of corroded specimen after 28 days, (c) XRD spectra of corroded specimen after 28 days, and (d) an SEM image of uncorroded specimen (before test).

(**Figure 15c**) revealed poorly crystalline corrosion products identified as magnetite (Fe$_3$O$_4$). In addition to Fe$_3$O$_4$, peaks corresponding to iron (Fe) were present suggesting a poor protective layer on the surface. The increase in carbon amount suggests that the metal surface may contain amorphous iron carbonate (FeCO$_3$).

For the MEA solution containing 4-aminobenzene sulfonic acid, the corrosion product was uniform over the metal surface similar to that found on the uninhibited surface (**Figure 16a**). Larger quantities of oxygen and carbon than in the uninhibited condition were observed from EDS spectra, indicating a significant amount of poorly protective corrosion product that was formed. This was confirmed by the XRD results, where peaks corresponding to Fe were characterized in addition to the primary corrosion product Fe$_3$O$_4$.

The presence of sulfapyridine and sulfolane led to tenacious surface layers on the metal surface. Fe$_3$O$_4$ was the primary corrosion product. The sulfapyridine induced a nonuniformly distributed corrosion product (**Figure 16b**) with large quantities of both oxygen and carbon observed from EDS and XRD spectra. The sulfolane led to a uniform intact surface layer (**Figure 16c**) with the least amounts of carbon and oxygen (**Figure 16d**) compared to the rest of inhibitors.

4.9. Performance comparison of tested corrosion inhibitors

Table 5 summarizes the performance of tested organic corrosion inhibitors. Five inhibitors, that is, 2-, 3-, and 4-aminobenzene sulfonic acids, sulfapyridine, and sulfolane showed promise for corrosion control in the MEA-based CO$_2$ absorption process. They could achieve up to 85–92%
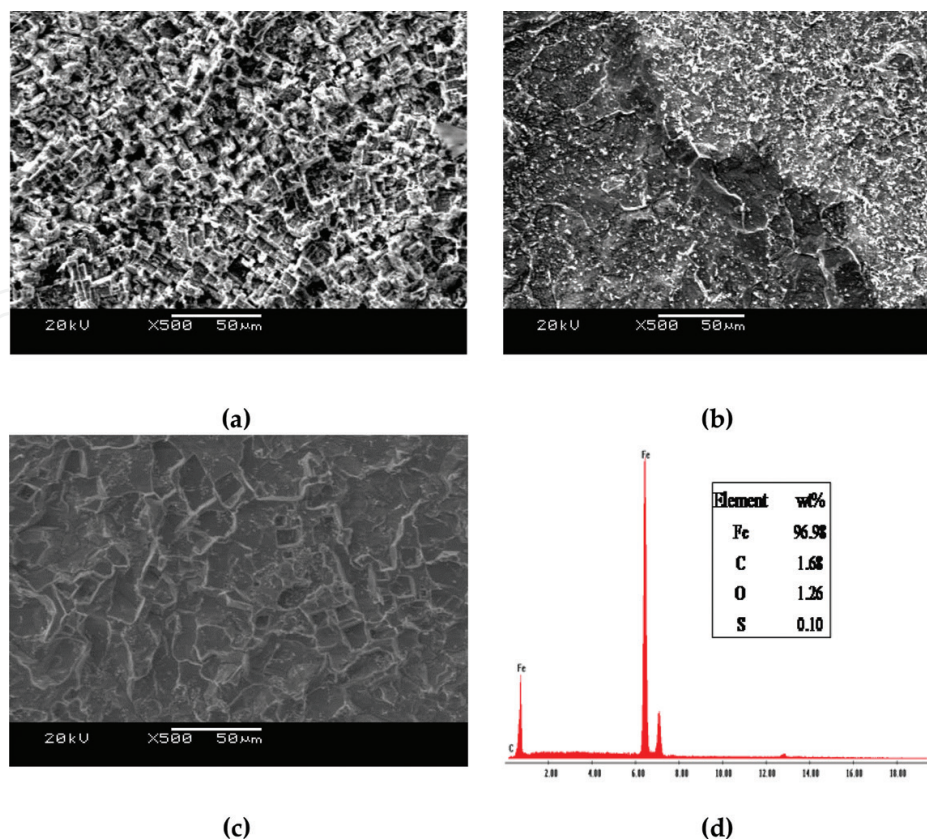
Figure 16. Surface analysis of tested specimen in inhibited solutions after 28 days (5.0 kmol/m^3 MEA, 80°C, and 0.55 mol/mol CO$_2$ loading): (a) SEM images (500× magnification) of 1000 ppm 4-aminobenzene sulfonic acid, (b) SEM images (500× magnification) of 2000 ppm sulfapyridine, (c) SEM images (500× magnification) of 2000 ppm sulfolane, and (d) EDS spectra of 2000 ppm sulfolane.

inhibition efficiency when applied at effective concentrations. The effective concentrations of 2-, 3-, and 4-aminobenzene sulfonic acid were in the range of 250–3000 ppm, while those of sulfapyridine and sulfolane were in higher ranges, that is, 3000–10,000 ppm and 2000–10,000 ppm, respectively. Reducing or increasing concentrations of these inhibitors from the effective concentration ranges may lessen their effectiveness.

Corrosion inhibitor	Effective concentration (ppm)	Inhibition efficiency (%)	Effective in chloride environment	Effective in formate environment
2-aminobenzene sulfonic acid	250–3000	87–89	Yes	No
3-aminobenzene sulfonic acid	250–3000	89	No (pitting)	No
4-aminobenzene sulfonic acid	250–3000	87–91	Yes	No
Sulfapyridine	3000–10,000	90–92	No	Yes
Sulfanilamide	(Not effective)	—	—	—
Sulfolane	2000–10,000	85–90	Yes	Yes
Thiosalicylic acid (incompatibility with MEA)	3000	80	—	—

Table 5. Performance summary of the tested organic corrosion inhibitors.

The effectiveness of most tested inhibitors was reduced when the MEA solution contained chloride or formate. 2- and 4-aminobenzene sulfonic acids can maintain their effectiveness in the presence of chloride but not in the presence of formate. On the contrary, sulfapyridine could function well in the presence of formate but not in the presence of chloride. The effectiveness of 3-aminobenzene sulfonic acid was lessened by both chloride (with possibility of pitting corrosion) and formate. Sulfolane was the only tested inhibitor that was not affected by chloride and formate.

Apart from the abovementioned inhibitors, two tested inhibitors were not promising. Sulfanilamide was not effective as it could only achieve up to 42% inhibition efficiency. Although thiosalicylic acid at 3000 ppm could achieve 80% inhibition efficiency, it was not compatible with the MEA solution.

5. Conclusions

2-, 3-, and 4-aminobenzene sulfonic acids, sulfapyridine, and sulfolane are effective corrosion inhibitors with inhibition efficiencies of up to 85–92%. Sulfolane is the most promising inhibitor compared to the other six tested compounds since it can yield up to 92% inhibition efficiency and maintain its effectiveness in the presence of both chloride and formate. 2- and 4-aminobenzene sulfonic acids do not work well in the presence of formate while sulfapyridine is not effective in the presence of chloride. 3-aminobenzene sulfonic acid can achieve up to 89%, but its effectiveness is deteriorated by both chloride and formate.

Acknowledgements

Author details

Sureshkumar Srinivasan, Amornvadee Veawab* and Adisorn Aroonwilas

*Address all correspondence to: veawab@uregina.ca

Energy Technology Laboratory, Faculty of Engineering and Applied Science, University of Regina, Saskatchewan, Canada

References

[1] Kohl AL, Nielsen RB. Gas Purification. 5th ed. Houston: Gulf Publishing Co.; 1997

[2] Mago BF, West CW. Antimony-vanadium corrosion inhibitors for alkanolamine gas treating system. US Patent 3808140; 1974

[3] Nieh ECY. Vanadium-amine corrosion inhibitor system for sour gas conditioning solutions. US Patent 4372873; 1983

[4] Pearce RL. Process for removal of carbon dioxide from industrial gases. US Patent 4440731; 1984

[5] Dupart MS, Oakes BD, Cringle DC. Method and composition for reducing corrosion in the removal of acidic gases from gaseous mixtures. US Patent 4446119; 1984

[6] Jones LW, Alkire JD. Corrosion inhibitors for amine gas sweetening systems. US Patent 4541946; 1985

[7] Hensen ER, Tipton TM, Courtwright JG. Corrosion inhibitors for alkanolamines. US Patent 4595723; 1986

[8] Srinivasan S. Environmentally friendly corrosion inhibitors for amine-based CO_2 absorption process [M.Sc. thesis]. Saskatchewan: University of Regina; 2012

[9] Hamah-Ali B, Ali BS, Yusoff R, Aroua MK. Corrosion of carbon steel in aqueous carbonated solution of MEA/[bmim] [DCA]. International Journal of Electrochemical Science. 2011;**6**:181-198

[10] Sastri VS. Corrosion Inhibitors: Principles and Applications. West Sussex: John Wiley & Sons Ltd.; 2001

[11] Hackerman N, Makrides AC. Action of polar organic inhibitors in acid dissolution of metals. Industrial and Engineering Chemistry. 1954;**46**(3):523-527

[12] Khaled KF, Hackerman N. Investigation of the inhibitive effect of *ortho*-substituted anilines on corrosion of iron in 1 M HCl solutions. Electrochimica Acta. 2003;**48**(19):2715-2723

[13] PubChem. 2011. Available from: http://pubchem.ncbi.nlm.nih.gov/ [Accessed: January 22, 2011]

[14] Chakrabarti A. Quantum chemical study of the corrosion inhibition of mild steel in 6 percent (wt/wt) HCl by means of cyanoguanidine derivatives. British Corrosion Journal. 1984;**19**:124-126

[15] Sastri VS, Perumareddi JR. Molecular orbital theoretical studies of some organic corrosion inhibitors. Corrosion. 1997;**53**(8):617-622

[16] Khalil N. Quantum chemical approach of corrosion inhibition. Electrochimica Acta. 2003; **48**(18):2635-2640

[17] Dupart MS, Bacon TR, Edwards DJ. Understanding corrosion in alkanolamine gas treating plants, part 1 & 2. Hydrocarbon Processing. 1993;**93**:75-80

[18] ASTM Standard G5-94 (Reapproved 2004). Standard reference test method for making potentiostatic and potentiodynamic anodic polarization measurements. In: Annual Book of ASTM Standards. West Conshohocken: American Society of Testing and Materials

[19] ASTM Standard G106-89 (Reapproved 2010). Standard practice for verification of algorithm and equipment for electrochemical impedance measurements. In: Annual Book of ASTM Standards. West Conshohocken: American Society of Testing and Materials

[20] Vračar LM, Dražić DM. Adsorption and corrosion inhibitive properties of some organic molecules on iron electrode in sulfuric acid. Corrosion Science. 2002;**44**(8):1669-1680